Dalton Transactions

ROYAL SOCIETY OF CHEMISTRY

PAPER

View Article Online
View Journal | View Issue

Cite this: *Dalton Trans.*, 2024, **53**, 12554

Synthesis and characterisation of copper(I) complexes with relevance to intramolecular Ullmann *O*,*S*-arylation†

Xiaodong Jin, [a,b] Bao-Nguyen T. Nguyen[a] and Robert P. Davies *[a]

Received 14th May 2024,
Accepted 6th July 2024

DOI: 10.1039/d4dt01418a

rsc.li/dalton

Copper-catalysed intramolecular Ullman arylation has been frequently used to synthesise benzoxazoles and benzothiazoles. Despite widespread use, investigations into the mechanism and speciation of copper-containing complexes relevant to the catalytic pathway have remained relatively limited. Accordingly, this study aims to elucidate the structural details of potential copper(I) intermediates through the analysis of their solid-state structures using X-ray crystallography, while also investigating the reactivities of these complexes. Five novel copper complexes are reported which are formed prior to the aryl halide activation step and feature distinct aggregation modes based on either $Cu_4N_4O_4C_4$ or $Cu_4N_4S_4C_4$ clusters.

Introduction

Benzoxazoles and benzothiazoles represent a valuable class of benzene-fused heterocycle that are often biologically active and prevalent in natural products and pharmaceuticals.[1–6] Their widespread use and importance has spurred a variety of synthetic routes to these compounds. Among these methods, copper-catalysed intramolecular arylation has garnered particular attention due to its high reactivity, cost-effectiveness in catalyst and ligand use, and its operation under mild conditions.[7,8] Various catalytic systems have been reported for this process including DMEDA/CuI,[9] 1,10-phenanthroline/CuI,[10–13] TMEDA/Cu salts,[14] oxazolidin-2-one/CuI,[15] methyl 2-methoxybenzoate/CuI,[16] 8-hydroxyquinoline/CuI,[17] an N-heterocyclic carbene/CuCl,[18] and trizoles/CuI[19–21] as well as a number of Cu(II) complexes[22–25] and CuO nanoparticles[26] (Scheme 1). Although significant progress has been made in developing more robust and efficient copper catalytic systems, the mechanism of the reaction and the identity of copper complexes in the catalytic cycle remains little explored.

The research reported herein aims to gain additional insight into the mechanism of copper(I)-catalysed intramolecular *O*- and *S*-arylation by analysing the solid-state structures of potential intermediary copper(I) species. These structures, prepared under air-free conditions and characterised by X-ray crystallography, offer insight into the range of interactions present between the metal centre and substrate, and builds upon previous studies in our group on the related intramolecular *N*-arylation reaction for the synthesis of benzimidazoles.[27]

Experimental

Materials

Anhydrous solvents such as dichloromethane, tetrahydrofuran, hexane, and toluene were obtained from a solvent tower using the PureSolv solvent purification system, degassed under N_2, and stored over molecular sieves. Anhydrous DMSO and dioxane were purchased in Sure/Seal™ bottles and used directly from the bottle. Deuterated solvents such as DMSO-d_6 and chloroform-d were purchased from Sigma-Aldrich or VWR and dried over 4 Å molecular sieves under N_2 before use. Copper(I) iodide (99.999% trace metals basis, powder) purchased from Sigma-Aldrich was stored in a glove box under N_2. All ligands and aryl halides were purchased from Sigma-

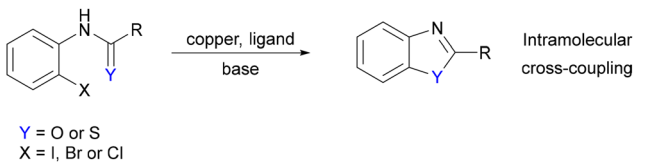

Scheme 1 Copper-catalysed intramolecular arylation.

[a]*Department of Chemistry, Molecular Sciences Research Hub, Imperial College White City Campus, Wood Lane, London W12 0BZ, UK. E-mail: r.davies@imperial.ac.uk*
[b]*Department of Chemistry, Xi'an Jiaotong-Liverpool University, Suzhou 215123, China*

†Electronic supplementary information (ESI) available: Additional experimental and crystallographic details. CCDC 2349373–2349378. For ESI and crystallographic data in CIF or other electronic format see DOI: https://doi.org/10.1039/d4dt01418a

Aldrich or VWR and used as received without further purification. For reactions that required air-free techniques, all glassware was pre-dried at 120 °C overnight and loaded in a glove-box under nitrogen. The experiments were carried out under a protective atmosphere of N_2.

General procedure for the synthesis of copper(I) complexes

A 4 mL vial was charged with mesitylcopper(I) (0.1 mmol) and aryl halides (0.1 mmol) fully dissolved in dry toluene (1.0 mL). The vial was placed inside a larger vial (20 mL) containing dry hexane (0.5 mL) and left at room temperature. Colourless crystals started to form in the inner vial after 24 h, and were isolated after 72 h.

$Cu_4$1a′$_4$. ^{1}H NMR (400 MHz, DMSO-d_6) δ 7.73 (s, 2H), 7.31 (dd, J = 7.9, 1.5 Hz, 1H), 7.26 (t, J = 7.3 Hz, 1H), 7.12 (t, J = 7.5 Hz, 3H), 7.02 (s, 1H), 6.96 (td, J = 7.6, 1.7 Hz, 1H). **Elemental analysis**: found 53.18; H 3.16; N 4.71. $C_{52}H_{36}Cl_4Cu_4N_4O_4$ requires 53.07 H 3.08; N 4.76%.

$Cu_4$2a′$_4$. ^{1}H NMR (400 MHz, DMSO-d_6) δ 7.40 (d, J = 8.0 Hz, 1H), 7.30–7.16 (m, 6H), 7.13–7.05 (m, 1H), 6.93 (d, J = 7.9 Hz, 1H). **Elemental analysis**: found C 53.86; H 3.41; N 4.23. $C_{52}H_{36}Cl_4Cu_4N_4S_4$ 1.3C_7H_8 requires 53.93; H 3.44; N 4.12%.

$Cu_4$2b′$_4$. ^{1}H NMR (400 MHz, DMSO-d_6) δ 8.21–8.04 (m, 3H), 7.66–7.42 (m, 4H), 7.33–7.09 (m, 2H). **Elemental analysis**: found C 44.02; H 2.56; N 3.95. $C_{52}H_{36}Br_4Cu_4N_4S_4$ requires C 44.02; H 2.72; N 3.80%.

$Cu_4$3a′$_4$. ^{1}H NMR (400 MHz, DMSO-d_6) δ 7.51–6.82 (m, 9H), 4.57 (s, 2H). **Elemental analysis**: found C 49.56; H 3.56; N 8.26. $C_{56}H_{48}Cl_4N_8S_4$ requires C 49.70; H 3.28; N 8.28%.

$Cu_4$3b′$_4$. ^{1}H NMR (400 MHz, DMSO-d_6) δ 8.64 (s, 1H), 7.70 (dd, J = 7.9, 1.3 Hz, 1H), 7.47–7.12 (m, 6H), 7.04 (td, J = 7.6, 1.2 Hz, 1H), 4.60 (d, J = 5.8 Hz, 2H); **Elemental analysis**: found C 43.91; H 3.13; N 7.30. $C_{56}H_{48}Br_4N_8S_4$ requires C 43.82; H 3.15; N 7.30%.

General procedure for the copper(I)-catalysed *O*-,*S*-arylation

A sample vial was charged with Cs_2CO_3 (0.15 mmol) and aryl halide (0.1 mmol) followed by addition of CuI solution (5 mol%), phenanthroline ligand when used (10 mol%) and internal standard naphthalene (0.05 mmol). The reaction was then stirred at 80 °C in DMSO-d_6 (1 mL) for 6 h. The mixture was cooled to room temperature and the clear organic layer was transferred into Young's type NMR tube under an N_2 atmosphere. The conversion and yield were determined by ^{1}H NMR and are tabulated in the results and discussion section.

2-Phenylbenzoxazole. ^{1}H NMR (400 MHz, chloroform-d) δ 8.27 (d, J = 4.0 Hz, 2H), 7.81–7.78 (m, 1H), 7.60–7.56 (m, 1H), 7.54–7.52 (m, 3H), 7.39–7.33 (m, 2H). **^{13}C NMR** (101 MHz, chloroform-d, ppm) δ 163.0, 150.8, 142.1, 131.5, 128.9, 127.6, 127.2, 125.1, 124.6, 120.0, 110.6.

2-Phenylbenzothiazole. ^{1}H NMR (400 MHz, chloroform-d) δ 8.11–8.09 (m, 3H), 7.88 (d, J = 8.0 Hz, 1H), 7.52–7.49 (m, 4H), 7.38 (t, J = 8.0 Hz, 1H). **^{13}C NMR** (101 MHz, chloroform-d) δ 168.1, 154.2, 135.2, 133.7, 131.1, 129.1, 127.6, 126.4, 125.3, 123.3, 121.7.

***N*-Benzyl-2-aminobenzo[*d*]thiazole. ^{1}H NMR** (400 MHz, chloroform-d) δ 7.60 (dd, J = 7.9, 1.2 Hz, 1H), 7.52 (d, J = 8.0 Hz, 1H), 7.45–7.26 (m, 6H), 7.11 (t, J = 7.2 Hz, 1H), 6.13 (br s, 1H), 4.66 (s, 2H). **^{13}C NMR** (101 MHz, chloroform-d) δ 167.9, 152.3, 137.6, 129.0, 128.0, 127.8, 126.2, 127.0, 121.8, 121.0, 119.0, 49.6.

Results and discussion

Isolation and characterisation of copper(I) complexes

In order to investigate possible mechanistic pathways for copper(I)-catalysed *O*- and *S*-arylations, a study into the solid-state structures of potential copper-containing intermediates was conducted. The precursors 2-halogenbenzanilide (**1**), 2-halogenthiobenzanilide (**2**) and (2-halogenphenyl)-benzylthiourea (**3**) were synthesised following published protocols.[28,29] With the starting materials in hand, single crystals were obtained from the reaction between the aryl halides and mesitylcopper(I), followed by recrystallisation of the resulting copper(I) complexes from toluene/hexane (Scheme 2).

The reaction employing **1a** as the reagent led to the isolation of a tetrameric complex Cu_4**1a**′$_4$ (where **1a**′ is deprotonated **1a**). Through X-ray crystallography, the structure of Cu_4**1a**′$_4$ was shown to adopt an unusual central $Cu_4N_4O_4C_4$ 16-membered folded ring, characterised by a slightly distorted rhombic Cu_4 core (Cu···Cu distances in the range of 2.6124(19) to 2.7445(6) Å; sum of interior angles 359.38°, Fig. 1a). The amide motif was deprotonated, giving a delocalized negative charge within the N–C–O unit. This was evident through the shorter C–N bonds (range from 1.3140(40) to 1.3257(40) Å) and longer C–O bonds (ranging from 1.2710(38) to 1.2837(34) Å) in Cu_4**1a**′$_4$, when compared to **1a**[30] (C–N: 1.3462(24) Å, C═O: 1.2305(18) Å).

The Cu_4**1a**′$_4$ structure contains two distinct copper(I) sites: one in which the copper is coordinated to two nitrogen atoms (Cu1 and Cu2 in Fig. 1a) and the other coordinated to two oxygen atoms (Cu3 and Cu4). Each Cu atom resides in a near-linear coordination environment, evident from N–Cu–N bond angles of 171.77° and 178.00°, and O–Cu–O bond angles of 162.82° and 165.72°. While several copper(I) complexes featuring planar Cu_4 arrangements and $Cu_4N_4O_4C_4$ 16-membered rings have been reported previously,[31–33] these tetrameric structures exhibited heteroligated N–Cu–O copper centres

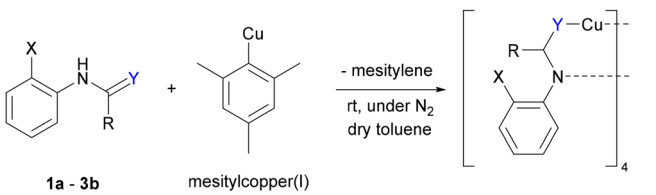

1a: Y = O; X = Cl; R = Ph **2a**: Y = S; X = Cl; R = Ph **3a**: Y = S; X = Cl; R = NHBn
1b: Y = O; X = Br; R = Ph **2b**: Y = S; X = Br; R = Ph **3b**: Y = S; X = Br; R = NHBn

Scheme 2 Synthesis of copper(I) complexes.

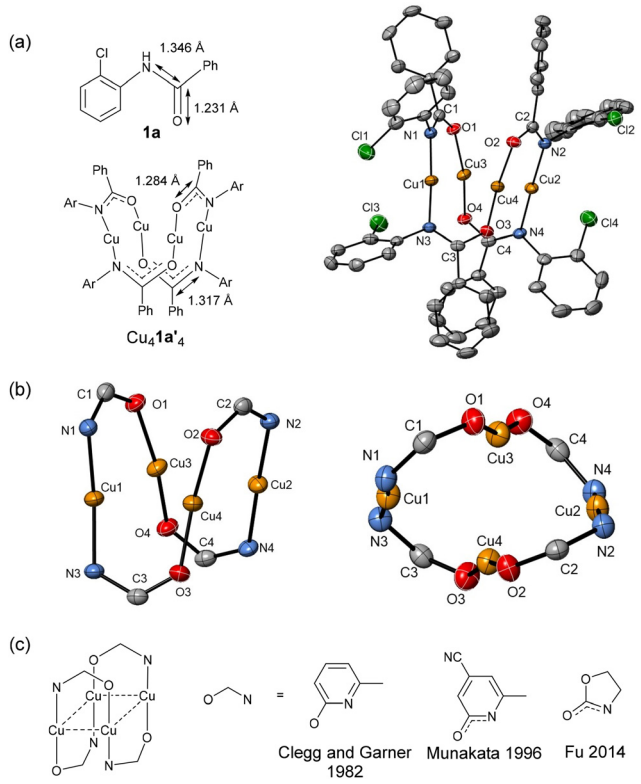

Fig. 1 (a) Solid-state structure of Cu_4**1a′**$_4$; thermal ellipsoids are set at 50% probability and hydrogen atoms are omitted for clarity. (b) Different views of the $Cu_4N_4O_4C_4$ 16-membered ring. (c) Cu(I) complexes containing a $Cu_4N_4O_4C_4$ 16-membered ring.[31–33]

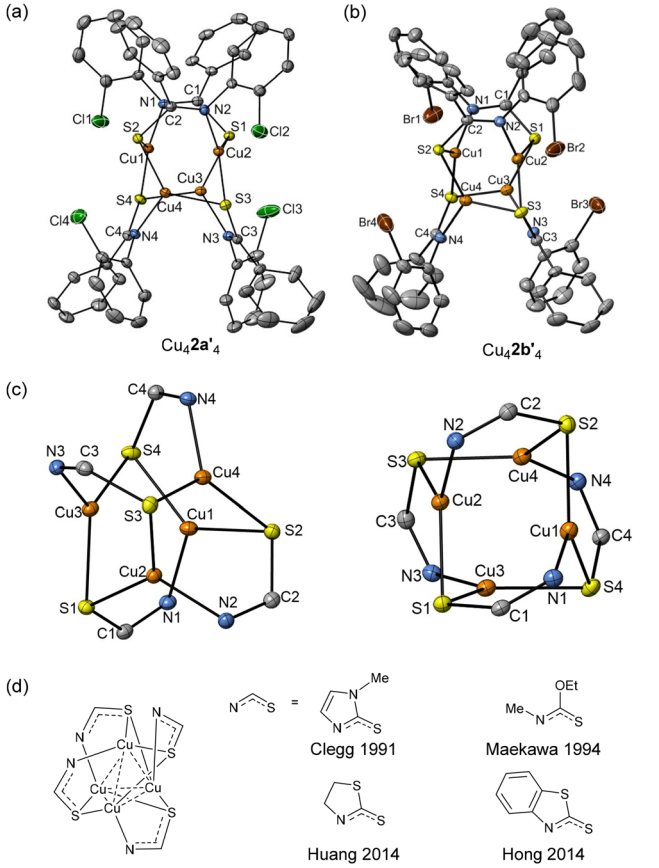

Fig. 2 (a) Solid-state structure of Cu_4**2a′**$_4$ (a) and Cu_4**2b′**$_4$ (b); thermal ellipsoids are set at 50% probability and hydrogen atoms are omitted for clarity. (c) Different views of the $Cu_4N_4S_4C_4$ 16-membered ring of Cu_4**2a′**$_4$. (d) Cu(I) complexes containing a $Cu_4N_4S_4C_4$ 16-membered ring.[35–39]

(Fig. 1c), in contrast to the distinct homoligated N–Cu–N and O–Cu–O units observed in this case.

The attempted reaction between aryl bromide **1b** and mesityl copper(I) did not yield single crystals suitable for X-ray diffraction analysis. However, the reaction of the thio analog, **2a**, with mesitylcopper(I) led to the formation of a copper(I) complex, the structure of which was elucidated through X-ray crystallography, revealing a tetrameric solid-state structure, Cu_4**2a′**$_4$. This structure comprises a central $Cu_4N_4S_4C_4$ cluster (Fig. 2a and c). In contrast to Cu_4**1a′**$_4$, Cu_4**2a′**$_4$ exhibits a tetrahedral Cu_4 core (Cu⋯Cu distances spanning 2.5170(26) to 2.9198(40) Å). Comparison of the bonding parameters between Cu_4**2a′**$_4$ and 3-chlorothiobenzanilide[34] (the solid-state structure of **2a** is currently unreported), highlighted the deprotonation of the thioamide and subsequent delocalization of the negative charge over the N–C–S unit (C–N: range 1.288(4)–1.300(4) Å; C–S: 1.755(3)–1.767(3) Å) compared to C–N 1.342 Å and C=S 1.671 Å in 3-chlorothiobenzanilide.

Each copper atom within the Cu_4 core is bonded to one nitrogen and two sulfur atoms, originating from three independent **2a′** molecules, thus giving a trigonal planar N–Cu-$(S)_2$ coordination motif. For example, Cu1 coordinates with N1, S2 and S4, exhibiting N1–Cu1–S2 angle of 113.92°, N1–Cu1–S4 angle of 116.52°, and S2–Cu1–S4 129.46°. The summation of these angles (359.91°) is consistent with the planarity of the N–Cu-$(S)_2$ unit. Correspondingly, the summed angles around Cu2, Cu3 and Cu4 are 359.84°, 360.00° and 359.96° respectively. The four copper centres are arranged in a tetrahedral configuration, exhibiting the shortest Cu⋯Cu distance of 2.5170(26) Å, which is shorter than the corresponding distances found in Cu_4**1a′**$_4$ (shortest Cu⋯Cu distance: 2.6124(19) Å). Furthermore, when aryl bromide **2b** was employed instead of aryl chloride **2a**, a tetramer structure Cu_4**2b′**$_4$ was obtained (Fig. 2b). The structure is analogous to Cu_4**2a′**$_4$ being also centred on a $Cu_4N_4S_4C_4$ polyhedron cluster and a tetrahedron Cu_4 core. The distances and angles closely resemble those observed in Cu_4**2a′**$_4$ (see ESI†). Several copper(I) complexes containing tetrahedron Cu_4 arrangements and $Cu_4N_4S_4C_4$ 16-membered rings have previously been reported and are summarised in Fig. 2d.[35–39] It is notable how a change from an amide (**1a**/**b**) to thioamide (**2a**/**b**) results in a significant change in the coordination geometries around the copper centres, likely facilitated by the increased tendency of the larger, softer sulphur atom to act as in a bridging capacity to copper(I) when compared to the amide oxygen atom in **1a**/**b**.

The thiourea substrates **3a/b** are of particular interest due to the presence of the additional NH group and the reported selectivity for the benzothiazole product over the mercaptobenzimidazole by-product on treatment with the Cu-catalyst. Thus, reaction of **3a** with mesitylcopper(I) led to the formation of a tetrameric aggregate, Cu_4**3a**′$_4$, whose solid-state structure was determined through X-ray crystallography (Fig. 3a). Cu_4**3a**′$_4$ shares similarities with Cu_4**2a**′$_4$, also containing a central Cu_4 tetrahedron (Cu···Cu distances in range 2.5742(24) to 2.8690 (13) Å). Comparison to the solid-state structure of **3a** obtained *via* recrystallisation of **3a** from toluene/hexane (see ESI†), showed deprotonation of the N_α–H of thiourea motif and charge delocalisation over the N_α–C–S unit. This was evidenced by the reduction in C–N bond lengths from 1.3565(39) Å in **3a** to 1.3062(67)–1.3074(71) Å in Cu_4**3a**′$_4$, along with an increase in C–S bond lengths from 1.6907(31) Å in **3a** to 1.7636(54)–1.7771(47) Å in Cu_4**3a**′$_4$. Furthermore, the amine group in the γ-position was not deprotonated and does not form any interactions with copper metal centres (**3a**: C–N_γ = 1.3338(50) Å; Cu_4**3a**′$_4$: C–N_γ = 1.3386(67)–1.3442(61) Å). This structural insight suggests a potential explanation for the selectivity observed between *S*-arylation and *N*-arylation in the Cu-catalysed cyclisation of (2-bromophenyl)-benzyl-thiourea (**3a**), as the copper is selectively coordinated to the N_α and S atoms. The synthesis of 2-mercaptobenzimidazoles through *N*-arylation usually requires an *S*-alkylation step to prevent the formation of C–S bonds.[40] Additionally, the utilisation of aryl bromide **3b** yielded a structurally similar tetrameric complex, Cu_4**3b**′$_4$ (Fig. 3b) with similar bond distances and angles to the chloride analogue (see ESI†). Once more, the copper selectively coordinated to the N_α and S atoms, while no interaction with N_γ was observed.

Reactivity of copper(I) complexes

To validate the plausibility of these copper(I) complexes as reaction intermediates, their reactivity was investigated by heating the complexes directly in DMSO-d_6 in order to obtain the final cyclised product. The resulting yields at varying temperatures are presented in Table 1, entries 1–5, along with the yields from the analogous catalytic reactions (entries 6–10). These complexes gave similar yield compared to that observed in catalytic reactions. Notably, reactions involving aryl chlorides required higher temperatures compared to those with aryl bromides as expected due to the higher aryl–halide bond strength. Furthermore, addition of an ancillary 1,10-phenanthroline ligand (**L1**) improved the final yields for both the stoichiometric and catalytic reactions. Addition of this ligand is thought to assist with lowering the aggregation state of the copper(I) clusters thus leading to an increase in reactivity,[27]

Table 1 The reactivity of Cu(I) complexes

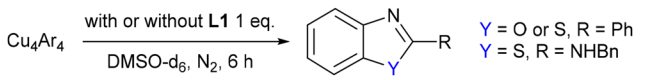

Entry	Substrate	Temp (°C)	Yield (%)	Yield with **L1** (%)
1	Cu_4**1a**′$_4$	130	26	96
2	Cu_4**2a**′$_4$	110	90	99
3	Cu_4**2b**′$_4$	80	97	99
4	Cu_4**3a**′$_4$	110	86	99
5	Cu_4**3b**′$_4$	80	96	99
	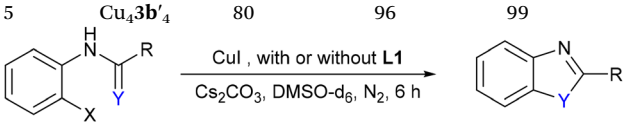			
6	**1a**	130	4	93
7	**2a**	110	58	99
8	**2b**	80	94	99
9	**3a**	110	72	99
10	**3b**	80	91	99

The reaction was carried out by heating the Cu(I) complexes Cu_4Ar_4 (0.1 mmol) in DMSO-d_6 (1 mL) with or without addition of **L1** (0.1 mmol). The comparison experiment was carried out by heating the aryl halides (0.1 mmol) using Cs_2CO_3 (0.15 mmol) as base in the presence of CuI (5 mol%) and **L1** (10 mol%). Yields were determined by ^{1}H NMR using naphthalene as internal standard.

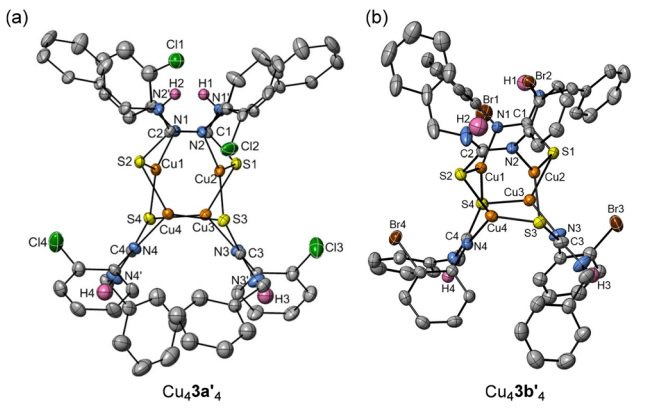

Fig. 3 Solid-state structure of Cu_4**3a**′$_4$ (a) and Cu_4**3b**′$_4$ (b); thermal ellipsoids are set at 50% probability and hydrogen atoms (except N_γ–H) are omitted for clarity.

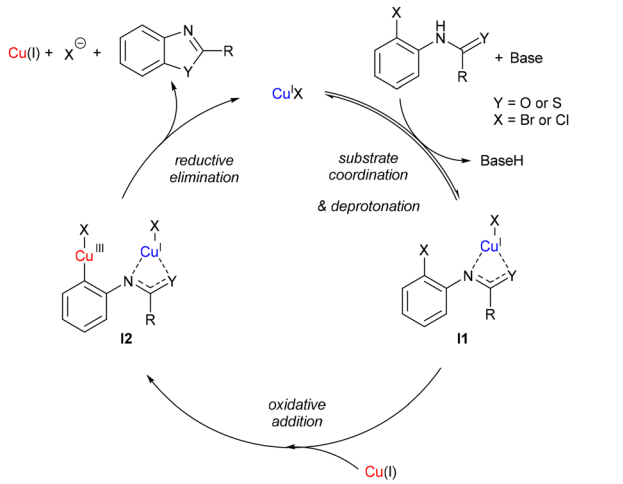

Scheme 3 Proposed mechanism for copper(I)-catalysed intramolecular *O*,*S*-arylation.

although our attempts to isolate related copper(I) complexes incorporating this ligand have so far been unsuccessful.

A putative mechanism based on the structural insights obtained in this work is proposed in Scheme 3. Based upon the observed distance between the copper(I) centres and aryl–halide bonds in the crystal structures, and also transposing the findings of our previously reported kinetic analysis on related copper-catalysed intramolecular *N*-arylation[27] two different copper centres are proposed to participate in the catalytic cycle. The aggregation state of the copper complexes in solution (DMSO) at high temperatures is likely to differ from those observed in the solid-state, and hence the complexes are shown as monomeric in the figure for simplicity.

Conclusions

Investigations into the solid-state structures of copper(I) complexes with selected organic amide and thioamide substrates have led to the observation of some novel copper(I) coordination complexes with unusual aggregation modes, and in addition offered insight into potential species present during intramolecular Ullmann *O*,*S*-arylation reactions. All copper(I) complexes exhibit amide deprotonation at the substrate N_α site and form tetrameric structures featuring $Cu_4Y_4N_4C_4$ (Y = O or S) central units. In the structures of thiourea complexes Cu_4**3a′**$_4$ and Cu_4**3b′**$_4$ the copper centres selectively coordinate with the N_α and S atoms, and no interactions with the N_γ atom are observed. This is congruent with the observed selectivity for *S*-arylation over *N*-arylation in the intramolecular cyclisation reaction. All copper complexes undergo intramolecular bond formation on heating in DMSO, yielding the desired cyclised products and making them viable intermediates or resting states in the intramolecular *O*,*S*-arylation reaction. Additionally, the introduction of 1,10-phenanthroline enhances the final yield, emphasising the positive impact of this ancillary ligand on the reaction outcome.

Data availability

The data supporting this article have been included as part of the ESI.†

Crystallographic data for all compounds have been deposited at Cambridge Crystallographic data centre (CCDC) under numbers 2349373–2349378 and can be obtained *via* **http://www.ccdc.cam.ac.uk/structures**. Additional information on the data refinements are included in the ESI.†

Conflicts of interest

There are no conflicts of interest to declare.

Acknowledgements

The authors gratefully acknowledge Dr Andrew White for help with collecting and solving the crystal structure data.

References

1 S. Soni, N. Sahiba, S. Teli, P. Teli, L. K. Agarwal and S. Agarwal, *RSC Adv.*, 2023, **13**, 24093–24111.
2 R. S. Keri, M. R. Patil, S. A. Patil and S. Budagumpi, *Eur. J. Med. Chem.*, 2015, **89**, 207–251.
3 S. Rajasekhar, B. Maiti and K. Chanda, *Synlett*, 2017, 521–541.
4 S. Noël, S. Cadet, E. Gras and C. Hureau, *Chem. Soc. Rev.*, 2013, **42**, 7747.
5 V. Facchinetti, R. da R. Reis, C. R. B. Gomes and T. R. A. Vasconcelos, *Mini-Rev. Org. Chem.*, 2012, **9**, 44–53.
6 A. Kamal, M. A. H. Syed and S. M. Mohammed, *Expert Opin. Ther. Pat.*, 2015, **25**, 335–349.
7 Q. Cai and W. Zhou, *Chin. J. Chem.*, 2020, **38**, 879–893.
8 Q. Yang, Y. Zhao and D. Ma, *Org. Process Res. Dev.*, 2022, **26**, 1690–1750.
9 G. Altenhoff and F. Glorius, *Adv. Synth. Catal.*, 2004, **346**, 1661–1664.
10 G. Evindar and R. A. Batey, *J. Org. Chem.*, 2006, **71**, 1802–1808.
11 R. D. Viirre, G. Evindar and R. A. Batey, *J. Org. Chem.*, 2008, **73**, 3452–3459.
12 Z. Luo, H. Wu, Y. Li, Y. Chen, J. Nie, S. Lu, Y. Zhu and Z. Zeng, *Adv. Synth. Catal.*, 2019, **361**, 4117–4125.
13 L. L. Joyce, G. Evindar and R. A. Batey, *Chem. Commun.*, 2004, 446–447.
14 N. Barbero, M. Carril, R. SanMartin and E. Domínguez, *Tetrahedron*, 2007, **63**, 10425–10432.
15 H. Ma and X. Jiang, *Synlett*, 2008, 1335–1340.
16 F. Wu, J. Zhang, Q. Wei, P. Liu, J. Xie, H. Jiang, B. Dai, S. Chang, C. Bolm, C. Tumanut, J. Li, G. Spraggon, J. Chang, T. Tuntland, J. L. Harris and D. S. Karanewsky, *Org. Biomol. Chem.*, 2014, **12**, 9696–9701.
17 D. Miao, X. Shi, G. He, Y. Tong, Z. Jiang and S. Han, *Tetrahedron*, 2015, **71**, 431–435.
18 J. I. Urzúa, R. Contreras, C. O. Salas and R. A. Tapia, *RSC Adv.*, 2016, **6**, 82401–82408.
19 A. S. Singh, M. Singh, N. Mishra, S. Mishra, A. K. Agrahari and V. K. Tiwari, *ChemistrySelect*, 2017, **2**, 154–159.
20 N. Mishra, A. S. Singh, A. K. Agrahari, S. K. Singh, M. Singh and V. K. Tiwari, *ACS Comb. Sci.*, 2019, **21**, 389–399.
21 M. Singh, P. Bose, A. S. Singh and V. K. Tiwari, *ChemistrySelect*, 2019, **4**, 9627–9631.
22 A. Naidu and G. Sekar, *Synthesis*, 2010, 579–586.
23 E. A. Jaseer, D. J. C. Prasad, A. Dandapat and G. Sekar, *Tetrahedron Lett.*, 2010, **51**, 5009–5012.
24 S. N. M. Boddapati, C. M. Kurmarayuni, B. R. Mutchu, R. Tamminana and H. B. Bollikolla, *Org. Biomol. Chem.*, 2018, **16**, 8267–8272.
25 Y. Tang, M. Li, H. Gao, G. Rao and Z. Mao, *RSC Adv.*, 2020, **10**, 14317–14321.

26 P. Saha, T. Ramana, N. Purkait, M. A. Ali, R. Paul and T. Punniyamurthy, *J. Org. Chem.*, 2009, **74**, 8719–8725.
27 X. Jin, Y. Lin and R. P. Davies, *Catal. Sci. Technol.*, 2023, **13**, 7181–7189.
28 E. Feng, H. Huang, Y. Zhou, D. Ye, H. Jiang and H. Liu, *J. Comb. Chem.*, 2010, **12**, 422–429.
29 D. Bernardi, L. Ba and G. Kirsch, *Synlett*, 2007, 2121–2123.
30 B. T. Gowda, B. P. Sowmya, J. Kozísek, M. Tokarcík and H. Fuess, *Acta Crystallogr., Sect. E: Struct. Rep. Online*, 2007, **63**, o2906.
31 M. Berry, W. Clegg, C. D. Garner and I. H. Hillier, *Inorg. Chem.*, 1982, **21**, 1342–1345.
32 L. P. Wu, M. Yamamoto, T. Kuroda-Sowa, M. Maekawa, Y. Suenaga and M. Munakata, *J. Chem. Soc., Dalton Trans.*, 1996, **23**, 2031.
33 H. Q. Do, S. Bachman, A. C. Bissember, J. C. Peters and G. C. Fu, *J. Am. Chem. Soc.*, 2014, **136**, 2162–2167.
34 G. Zhao, *Acta Crystallogr., Sect. E: Crystallogr. Commun.*, 2015, **71**, o353.
35 D. M. Knotter, M. D. Janssen, D. M. Grove, W. J. J. Smeets, E. Horn, A. L. Spek and G. Van Koten, *Inorg. Chem.*, 1991, **30**, 4361–4366.
36 E. S. Raper, J. R. Creighton and W. Clegg, *Inorg. Chim. Acta*, 1991, **183**, 179–187.
37 T. Kuroda-Sowa, M. Munakata, M. Miyazaki and M. Maekawa, *Acta Crystallogr., Sect. C: Cryst. Struct. Commun.*, 1994, **50**, 1026–1028.
38 J.-M. Du, H.-Y. Zeng, Z.-C. Dong, G. C. Guo and J.-S. Huang, *Acta Crystallogr., Sect. C: Cryst. Struct. Commun.*, 2002, **58**, m396–m397.
39 C. Yue, C. Yan, R. Feng, M. Wu, L. Chen, F. Jiang and M. Hong, *Inorg. Chem.*, 2009, **48**, 2873–2879.
40 S. Murru, B. K. Patel, J. Le Bras and J. Muzart, *J. Org. Chem.*, 2009, **74**, 2217–2220.